The Astrophysical Journal, 455:L139–L142, 1995 December 20

A BLACK HOLE IN THE X-RAY NOVA GS 2000+25[1]

Alexei V. Filippenko, Thomas Matheson, and Aaron J. Barth
Department of Astronomy, University of California at Berkeley, Berkeley, CA 94720; afilippenko, tmatheson, abarth@astro.berkeley.edu
Received 1995 August 11; accepted 1995 October 3

ABSTRACT

We have obtained 13 moderate-resolution (~2.5 Å) spectra of the Galactic X-ray nova GS 2000+25 in quiescence with the W. M. Keck 10 m telescope. Cross-correlation with the spectra of late-type dwarfs (especially K2–K7) yields excellent radial velocities for the secondary star. The orbital period is consistent with that previously obtained from photometry (~8.3 hr). A semiamplitude of 518.4 ± 3.5 km s^{-1} is found, ~25% smaller than the outer disk velocity implied by the double-peaked Hα emission line ($\Delta v/2 \approx 700$ km s^{-1}). The derived mass function is 4.97 ± 0.10 $M_\odot$, the second highest known for any low-mass X-ray binary. Being considerably above the conventional limiting mass for a neutron star (~3.2 $M_\odot$), it strongly suggests that the compact primary is a black hole. Plausible mass estimates based on $M_2 = 0.4$–$0.7\ M_\odot$ and $i = 67.^\circ5$–80° are $M_1 = 5.9$–$7.5\ M_\odot$. Under the assumption that the radial velocity curve of the centroid of the Hα emission line represents the true motion of the black hole, we formally find $q = M_2/M_1 = 0.050 \pm 0.026$.

Subject headings: binaries: close — black hole physics — novae, cataclysmic variables — stars: individual (GS 2000+25) — X-rays: stars

1. INTRODUCTION

On 1988 April 26 UT, a bright, transient X-ray source was discovered with the All-Sky Monitor aboard the *Ginga* satellite (Tsunemi et al. 1989). This "X-ray nova," designated GS 2000+25, was also visible in prediscovery *Ginga* observations (April 23–25) obtained with the Large Area Counter. Its spectral and temporal characteristics were similar to those of previously observed ultrasoft X-ray transients, which might be black holes in binary systems (White, Nagase, & Parmar 1995; van Paradijs & McClintock 1995; Tanaka & Lewin 1995; references therein).

GS 2000+25 had an optical counterpart of $V = 16.4$ mag at maximum (Nova Vul 1988; QZ Vul). A spectrum (Charles et al. 1991) revealed Hα and He II λ4686 emission lines superposed on a highly reddened continuum [$E(B-V) = 1.1$–1.7 mag]. Optical photometry after outburst and during quiescence suggests an orbital period of 8.25836 ± 0.00012 hr (Chevalier & Ilovaisky 1993, hereafter CI93). There is also good evidence of ellipsoidal modulation, and the tidally distorted secondary star is likely to be a late-type (K or G) dwarf (Callanan & Charles 1991; CI93).

Accurate masses for the compact objects in X-ray transients can be obtained during quiescence by monitoring the absorption lines in spectra of the secondary star, but this is difficult if the secondary is a faint dwarf. Images of GS 2000+25 obtained on 1995 June 27 with the Lick 1 m Nickel reflector yield $R \approx 21.2$ mag, consistent with previously published values and comparable to the magnitude of the X-ray nova GRO J0422+32 (V518 Per) when Filippenko, Matheson, & Ho (1995, hereafter FMH) measured its mass function with the W. M. Keck 10 m telescope. Inspired by this success, we decided to observe GS 2000+25 in a similar manner. Here we present our data and results.

2. OBSERVATIONS AND REDUCTIONS

GS 2000+25 was observed with the Low Resolution Imaging Spectrometer (LRIS; Oke et al. 1995) at the Cassegrain focus of the Keck I telescope during the night of 1995 July 22 UT; a journal of observations is given in Table 1. The sky was clear, and the atmospheric seeing was generally 0."8–1."0. We used a Tektronix 2048 × 2048 pixel CCD with a scale of 0."205 pixel^{-1} (0."41 per binned pixel in the spatial direction), a gain of 1.1 e count^{-1}, and a readout noise of 6 e pixel^{-1}.

The long slit of width 1" was oriented at a position angle of 50.°2 to include the two stars roughly 5" and 12" northeast of GS 2000+25 (see the finding chart published by Chevalier & Ilovaisky 1990). These were used to monitor possible variations in the flux of the nova and to test for systematic shifts in the wavelength scale as a function of hour angle. Emission-line comparison lamps (Hg-Ne) were observed after each pair of nova spectra, as well as before the first pair. Our average FWHM resolution was ~2.5 Å (~120 km s^{-1}) over a wavelength range of ~5640–6940 Å, comparable to the values in FMH. Twelve velocity standards with spectral types in the range G5 V–M0 V were observed in twilight with the same setup, as were two sdF stars (Oke & Gunn 1983) for flux-calibration and removal of telluric absorption lines.

Cosmic rays were eliminated from the two-dimensional spectra through comparison of pairs of consecutive exposures. We used the APALL task in IRAF to optimally extract (Horne 1986) one-dimensional, sky-subtracted spectra. The typical signal-to-noise ratio per final 0.75 Å bin is ~7 in the continuum.

The spectra of GS 2000+25 consist of a red continuum on which are superposed Hα and very weak He I λ5876 emission lines; see Figure 1. (Note that the red peak of He I coincides with the strong Na I D absorption line.) Significant changes were visible in the Hα profile during the course of the night, but the basic double-peaked structure ($\Delta v \approx 1400$ km s^{-1}) remained clear. The Hα equivalent width (EW; average value 40 ± 5 Å) was always much smaller than that of GRO J0422+32 (EW ≈ 250 Å; FMH).

3. ANALYSIS

3.1. *Cross-Correlations*

We employed the FXCOR package ("Release 9/13/93") in IRAF to cross-correlate the spectra of GS 2000+25 with the

[1] Based on observations obtained with the W. M. Keck Observatory.

TABLE 1

JOURNAL OF OBSERVATIONS AND RADIAL VELOCITIES

HJD[a]	Exp. (s)	Airmass[b]	Phase[c]	v_2 (km s^{-1})[d]	v_1 (km s^{-1})[e]
9920.8028	2400	1.37	0.61313	−357.7 ± 10.3	6.99 ± 96.75
9920.8313	2400	1.21	0.69587	−115.6 ± 9.31	61.12 ± 27.15
9920.8622	2100	1.10	0.78567	174.8 ± 13.5	69.94 ± 25.09
9920.8854	1800	1.04	0.85329	348.5 ± 7.51	41.16 ± 32.35
9920.9115	1500	1.01	0.92897	536.2 ± 6.84	72.27 ± 30.16
9920.9313	1800	1.00	0.98648	533.0 ± 5.48	2.70 ± 45.92
9920.9570	1800	1.01	0.06114	506.9 ± 6.65	8.68 ± 43.08
9920.9785	1800	1.04	0.12371	415.1 ± 6.37	12.15 ± 39.99
9921.0021	1800	1.09	0.19232	226.6 ± 11.2	7.95 ± 39.62
9921.0236	1800	1.16	0.25489	60.03 ± 8.81	25.30 ± 32.12
9921.0472	1800	1.27	0.32351	−224.8 ± 14.4	19.09 ± 39.59
9921.0705	2100	1.44	0.39113	−369.7 ± 7.21	23.53 ± 40.72
9921.1021	2400	1.79	0.48294	−478.3 ± 6.50	39.79 ± 37.46

[a] HJD − 2,440,000 at midpoint of exposure.
[b] Airmass at midpoint of exposure.
[c] Using $P = 0.344098$ days and $T_0 = 9920.93590$.
[d] Secondary-star radial velocity.
[e] Hα centroid radial velocity, from fit to emission-line wings.

12 velocity standards; see FMH for details. The correlation was performed over the range 5950–6520 Å. In all cases a definitive correlation peak was obvious. Typical values of the Tonry & Davis (1979) significance threshold were quite high, $R \approx 4$. As in FMH, we adopted the FXCOR uncertainties reduced by a factor of 2.77, but we suspect that these might be too small (see below).

The strongest correlation was obtained with BD −05°3763, a K5 V star, but that with BD −03°3746 (K4 V) was nearly identical. Dwarfs in the range G5–K1 and K8–M0 also gave very good correlations. Using the radial velocities evaluated from the correlations with BD −05°3763 (corrected for the radial velocity of BD −05°3763 itself, −46.1 km s^{-1}), we conducted a least-squares fit to obtain the best cosine curve to match the data (Fig. 2). The period was fixed to be that reported by CI93 (0.344098 days). The three-parameter fit (zero point, semiamplitude, and phase) yielded a systemic velocity of $\gamma_2 = 36.2 \pm 2.6$ km s^{-1}, a semiamplitude of $K_2 = 518.4 \pm 3.5$ km s^{-1}, and a starting time (Heliocentric Julian Date) for the phase of T_0 = HJD 2,449,920.93590 ± 0.00039, where T_0 is defined as the point of maximum *redshifted* velocity.[2] A better measurement of the systemic velocity is $\gamma_2 = 30.6 \pm 4.3$ km s^{-1}, the mean of results obtained with the eight standard stars having the highest R-values.

When the fit was recomputed with the period as an additional free parameter, we found $P = 0.3516 \pm 0.0034$ days. This is consistent with (but 2.2 σ longer than) the photometric value of CI93, removing any remaining doubts that the latter corresponds to the orbital period. Specifically, it is inconsistent with the period proposed by Shahbaz et al. (1994b; 0.2935 days). We adopt the

[2] The two points at phase 0.92 and 0.99 (Fig. 2) were excluded from the fit, but the results are not significantly affected by this; inclusion of them gives $\gamma_2 = 35.8 \pm 2.6$ km s^{-1}, $K_2 = 516.5 \pm 2.9$ km s^{-1}, and T_0 = HJD 2,449,920.93565 ± 0.00038. These points have among the smallest formal error bars, yet they fall far off the cosine curve. Since the telescope at that time was close to the meridian, the spectrograph was rotating rapidly; the wavelength scales may therefore be slightly erroneous, although no obvious problems were seen in the positions of night-sky emission lines.

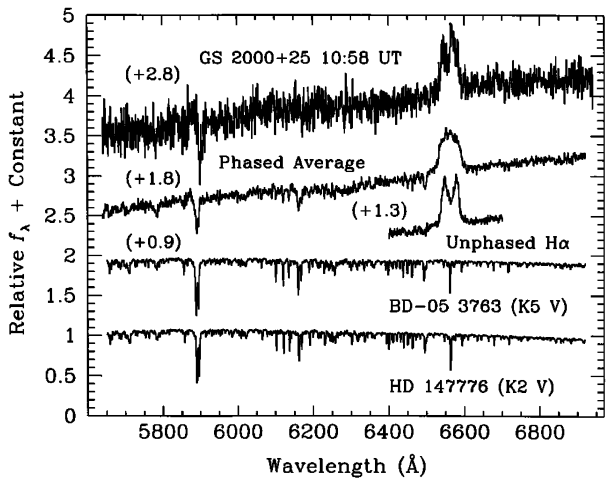

FIG. 1.—Spectra of GS 2000+25 compared with scaled spectra of two velocity standards (K5 V and K2 V). Constants have been added to the top four spectra for clarity. The typical spectrum (*top*) of GS 2000+25 was taken at 10:58 UT (midpoint of observation). The rest-frame ("phased average") spectrum of the secondary star was obtained by averaging all 13 exposures after Doppler-shifting each to zero velocity. Note that this procedure smears out features associated with the accretion disk around the compact primary (most notably Hα emission), as well as interstellar absorption lines. An unphased average of the spectra (*middle*) clearly shows the double-peaked Hα profile.

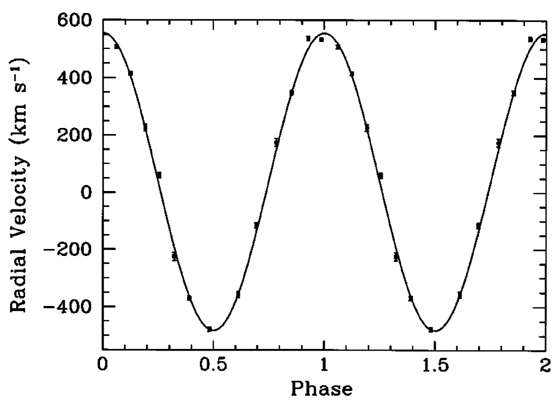

FIG. 2.—Radial-velocity curve of the secondary star in GS 2000+25, derived from cross-correlations of individual spectra with those of the K5 V star BD −05°3763. The radial velocity of the comparison star, −46.1 km s^{-1}, has been added to all values. The orbital period is 0.344098 ± 0.000005 days. Formal error bars are 1 σ, but these are too small, as indicated by the high value of $\chi^2_\nu = 5.0$.

determination of CI93 because it is based on observations of many orbits rather than just one as in our own data.

All the uncertainties quoted above are the formal 1 σ values derived from the least-squares fit. The reduced χ^2 (χ^2_ν) for the best fit is 5.0, not especially good. However, the true value is probably lower; indeed, Tonry & Davis (1979) explicitly pointed out that the velocity uncertainties usually will need to be adjusted to reflect the external errors in the data. In our case, $\chi^2_\nu \approx 1.5$ if the velocity uncertainties are actually 50% larger.

The points in Figure 2 have much smaller uncertainties than those obtained for GRO J0422+32 by FMH, yet the objects have comparable R-band magnitudes. There are two main reasons for this: (1) Contamination by the accretion disk is smaller in GS 2000+25 than in GRO J0422+32 (§ 3.2); hence, the absorption lines suffer less dilution, and Hα emission contributes less to the R-band flux. (2) The atmospheric seeing was generally better, and the CCD readout noise was lower, during the GS 2000+25 observations.

3.2. *Averaged Spectrum*

We obtained the master "rest-frame" spectrum (t = 7.1 hr) of the secondary star by averaging all 13 individual spectra after Doppler-shifting each one to zero velocity. Figure 1 shows the averaged spectrum in comparison with spectra of K5 V and K2 V velocity standards. There is a clear correspondence between the stellar absorption lines. It is very difficult to determine which comparison star is most appropriate; early to mid-K dwarfs exhibit nearly identical spectra in the observed wavelength range.

The absorption lines in GS 2000+25 appear somewhat weaker than those in the standard stars. While this could indicate that the spectral type of the secondary is substantially earlier than K2, tests show that line broadening and contamination by the featureless continuum of an accretion disk are likely to be the most important factors. There are two contributions to the broadening. First, with a possible mass ratio $q = M_2/M_1 \approx 0.050$ (§ 4), the rotational broadening (see, e.g., Wade & Horne 1988) is expected to be $v \sin i = 0.462\, K_2 q^{1/3}(1+q)^{2/3} \approx 90$ km s^{-1}. (This rises to 120 km s^{-1} if $q \approx 0.1$.) Second, the motion of the secondary star during a given exposure (T) smears the lines by up to $2\pi K_2 T/P$ km s^{-1}. In our case (T = 1800 s) this amounts to ~200 km s^{-1}. Even a typical value for the smearing ($4K_2T/P \approx 130$ km s^{-1}) is comparable to the spectral resolution. A preliminary estimate of the contribution of the accretion disk (10%–20% of the continuum at 6300 Å) was obtained by comparing broadened and diluted spectra of velocity standards with the averaged spectrum of GS 2000+25.

A prominent absorption line of Li I λ6708 is present in our spectrum (Fig. 2): EW = 0.27 ± 0.04 Å. Unexpectedly strong Li I λ6708 absorption (EW = 0.25–0.48 Å) is also seen in the spectra of several other X-ray novae (see Martín et al. 1994 and references therein). Its narrow width indicates an association with the secondary star, yet the atmospheres of old dwarfs should have extremely low Li abundance due to mass loss via accretion and to burning in deeper, convectively mixed layers. The outbursts of X-ray novae may produce the excess Li, but the exact mechanism is unknown.

3.3. Hα *Measurements*

The middle spectrum of Figure 1 illustrates the nearly symmetric Hα emission profile obtained from a straight (i.e., unphased) average of all 13 spectra. It resembles that of several other Galactic X-ray novae (see, e.g., Orosz et al. 1994) with well-separated double peaks. An approximate fit was achieved with a thin accretion disk model (Smak 1981) having $\alpha \approx 1.5$ (the power-law exponent for the density function of the emitting atoms), $K_d \approx 700$ km s^{-1} (the projected velocity of the outer disk), and $r_1 \approx 0.1$ (the ratio of the inner to outer radii of the disk). Note that $K_d \approx 0.74\, K_2$, somewhat smaller than found in A0620−00 and Nova Mus 1991 by Orosz et al.

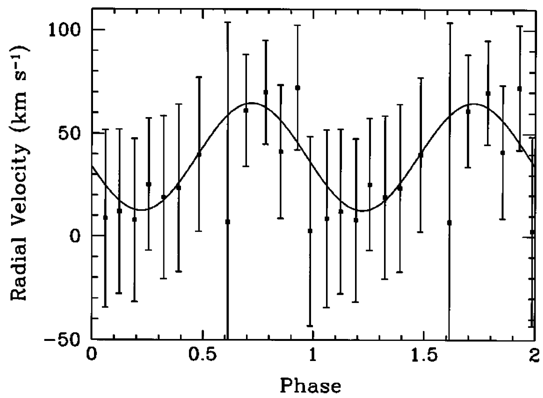

FIG. 3.—Radial-velocity curve of the centroid of the Hα emission line, determined by fitting a Gaussian to the high-velocity wings. The period was forced to be 0.344098 days, as for the secondary star; all other parameters were allowed to vary. Formal error bars are 1 σ, but these appear to be too large.

To investigate the motion of the compact primary, we fitted a Gaussian to the high-v wings ($v \approx 800$–2800 km s^{-1}) of the Hα line in each individual spectrum using the IRAF task SPECFIT. The regions of the fit (including the continuum) were 6400–6545 Å and 6580–6710 Å; the double-horned core of the line was excluded. The velocity of the Gaussian peak and its formal 1 σ uncertainty were adopted for each spectrum.

As shown in Figure 3, the derived velocity tends to be low in the first half of the orbit and high in the second half, perhaps suggesting periodic behavior. We used a least-squares fit to determine the Hα radial-velocity cosine curve, forcing the data to have the period found by CI93 (0.344098 days) but allowing all other parameters to vary. The formal results (Fig. 3) are as follows: $\gamma_1 = 38 \pm 10$ km s^{-1}, $K_1 = 26 \pm 13$ km s^{-1}, and a zero point in the phase of HJD 2,449,921.1843 ± 0.03329 days. Within the uncertainties, this value of γ_1 is consistent with γ_2.

Once again, the zero point of the phase is the maximum *redshifted* velocity; it implies that the compact object is 260° out of phase with the secondary star, rather than 180° as expected. This is close to the phase offset of 253° found by FMH in GRO J0422+32. Similar phase shifts are seen in the Galactic black hole candidates A0620−00 and Nova Mus 1991 (Orosz et al. 1994). These distortions suggest that the accretion disk often has a nonaxisymmetric distribution of surface brightness or noncircular velocities, and they cast some doubt on the use of Hα radial-velocity curves to determine the motion and mass of the primary star. On the other hand, Orosz et al. pointed out that the values of K_1 and the mass ratio q found from their Hα radial-velocity curve of A0620−00 are consistent with those determined with independent techniques.

4. MASS OF THE COMPACT PRIMARY

From the semiamplitude ($K_2 = 518.4 \pm 3.5$ km s^{-1}) and period ($P = 0.344098 \pm 0.000005$ days; CI93) of the radial-velocity curve of the secondary star, we find a mass function $f(M) = PK_2^3/2\pi G = 4.97 \pm 0.10\ M_\odot$. Of all low-mass X-ray binaries, this is the second largest known mass function; it is exceeded only by GS 2023+338, with $f(M) = 6.08 \pm 0.06\ M_\odot$ (Casares & Charles 1994). Our value for GS 2000+25 can be compared with that of Charles & Casares (1995), who reported $f(M) = 4.2 \pm 0.5\ M_\odot$ ($K_2 = 490 \pm 22$ km s^{-1}) on 1995 July 28, 1 week after our data were obtained.

The *absolute minimum* mass of the compact primary is therefore 4.97 $M_\odot$. Since $f(M) = M_1^3 (\sin^3 i)/(M_1 + M_2)^2$, a more realistic lower limit is 6.2 $M_\odot$ if the secondary is a *normal* K5 dwarf ($M_2 \approx 0.7\ M_\odot$; Allen 1976). Since neither X-ray eclipses (Shahbaz et al. 1994b) nor optical eclipses (CI93; this paper) were seen, the inclination is probably less than 80°; hence, the minimum value of M_1 further increases to 6.4 $M_\odot$. Alternatively, if the secondary is *less* massive than implied by its spectral type, as in some X-ray binaries (see, e.g., van den Heuvel 1983), then the minimum mass is smaller; with $M_2 = 0.4\ M_\odot$ (a reasonable lower limit), we find $M_1 = 5.7\ M_\odot$ ($i = 90°$) and $M_1 \gtrsim 5.9\ M_\odot$ ($i \lesssim 80°$).

The measured semiamplitude of the radial velocity curve of the primary ($K_1 = 26 \pm 13$ km s^{-1}), *if reliable*, can be used in conjunction with our value of K_2 to obtain a mass ratio $q = 0.050 \pm 0.026$. Hence, *if* the secondary is a normal K5 dwarf, then the mass of the primary is $M_1 = 14 \pm 7\ M_\odot$. Moreover, the inclination angle of the system can be obtained from $f(M)$, M_1, and M_2: $\sin^3 i = f(M)(M_1 + M_2)^2/M_1^3$; formally, we find $i = 48° \pm 11°$. However, the inclination derived from the ellipsoidal modulations is $\gtrsim 67\overset{\circ}{.}5$ (CI93), substantially higher. Adopting this constraint, together with $i \lesssim 80°$, we obtain $M_1 = 5.9$–$7.0\ M_\odot$ (if $M_2 \approx 0.4\ M_\odot$) or $M_1 = 6.4$–$7.5\ M_\odot$ (if $M_2 \approx 0.7\ M_\odot$).

When we calculate the effective Roche lobe radius (R_L) of the secondary star from the relation of Paczyński (1971; see also Eggleton 1983) and Kepler's third law, we find that $R_L = 0.85\ R_\odot$ if $M_2 \approx 0.7\ M_\odot$. This is ~15% greater than the expected radius of a normal K5 dwarf ($R = 0.74\ R_\odot$; Allen 1976). A less massive main-sequence secondary gives an even larger discrepancy. Thus, it is difficult to see how the mass transfer leading to the X-ray outburst could have occurred unless the secondary is somewhat evolved. Since isolated K5 V stars have an evolutionary timescale longer than the Hubble time, this suggests that the secondary began its life as a more massive star and subsequently lost considerable mass through interactions with the primary. Its current mass may well be less than 0.7 $M_\odot$, as noted above.

5. CONCLUSIONS

The maximum gravitational mass of a slowly rotating neutron star is widely believed to be 3.0–3.2 $M_\odot$ (e.g., Chitre & Hartle 1976; see discussion in FMH). Observations of neutron stars in binary systems almost always yield $M = 1.0$–$1.8\ M_\odot$ (Thorsett et al. 1993). The mass function we have determined for GS 2000+25, 4.97 $M_\odot$, is comfortably above these values. The actual minimum mass (adopting $i \lesssim 80°$ and $M_2 \gtrsim 0.4\ M_\odot$) is 5.9 $M_\odot$, even further above the conventional mass limit. Under the *assumptions* that $M_2 \approx 0.7\ M_\odot$ (a normal K5 V star) and that $q = M_2/M_1 \approx 0.05$ (as suggested by our Hα radial-velocity curve), the implied mass of the compact object is ~14 $M_\odot$, but in this case $i = 48° \pm 11°$. Given the plausibility of an undermassive secondary and a larger inclination, a more realistic estimate is $M_1 \approx 5.9$–$7.5\ M_\odot$. This is larger than many (but not all) extreme models of neutron stars that include rapid rotation (Friedman & Ipser 1987) or nonstandard equations of state (Bahcall, Lynn, & Selipsky 1990).

Thus, it is very likely that the compact primary in GS 2000+25 is a black hole. Indeed, this is now one of the best black hole candidates, second only to GS 2023+338 (Casares & Charles 1994) among low-mass X-ray binaries, and less model-dependent than famous high-mass X-ray binaries such as Cyg X-1 (see, e.g., van Paradijs & McClintock 1995 and references therein). Further progress will be made with a more secure estimate of the inclination of the system, which can be deduced from detailed modeling of ellipsoidal brightness variations at infrared wavelengths (see, e.g., Shahbaz et al. 1994a, for GS 2023+338). We recently obtained the necessary data for such an analysis.

The W. M. Keck Observatory, made possible by the generous and visionary gift of the W. M. Keck Foundation, is operated as a scientific partnership between the California Institute of Technology and the University of California. We thank R. Campbell, S. Doyle, and T. Stickel for their assistance and the LRIS instrument team (led by J. G. Cohen) for their recent upgrade of the spectrograph. J. Orosz kindly sent lists of velocity-standard stars, and J. Anderson provided his algorithm for the removal of cosmic rays. We are grateful to S. Van Dyk and D. Leonard for obtaining optical images of GS 2000+25 in 1995 June. This work was supported by the NSF through grant AST-9417213.

REFERENCES

Allen, C. W. 1976, Astrophysical Quantities (3d ed.; London: Athlone)
Bahcall, S., Lynn, B. W., & Selipsky, S. B. 1990, ApJ, 362, 251
Callanan, P. J., & Charles, P. A. 1991, MNRAS, 249, 573
Casares, J., & Charles, P. A. 1994, MNRAS, 271, L5
Charles, P. A., & Casares, J. 1995, IAU Circ. 6193
Charles, P. A., Kidger, M. R., Pavlenko, E. P., Prokofieva, V. V., & Callanan, P. J. 1991, MNRAS, 249, 567
Chevalier, C., & Ilovaisky, S. A. 1990, A&A, 238, 163
———. 1993, A&A, 269, 301 (CI93)
Chitre, D. M., & Hartle, J. B. 1976, ApJ, 207, 592
Eggleton, P. P. 1983, ApJ, 268, 368
Filippenko, A. V., Matheson, T., & Ho, L. C. 1995, ApJ, 455, 614 (FMH)
Friedman, J. L., & Ipser, J. R. 1987, ApJ, 314, 594
Horne, K. 1986, PASP, 98, 609
Martín, E. L., Rebolo, R., Casares, J., & Charles, P. A. 1994, ApJ, 435, 791
Oke, J. B., et al. 1995, PASP, 107, 375
Oke, J. B., & Gunn, J. E. 1983, ApJ, 266, 713
Orosz, J. A., Bailyn, C. D., Remillard, R. A., McClintock, J. E., & Foltz, C. B. 1994, ApJ, 436, 848
Paczyński, B. 1971, ARA&A, 9, 183
Shahbaz, T., Ringwald, F. A., Bunn, J. C., Naylor, T., Charles, P. A., & Casares, J. 1994a, MNRAS, 271, L10
Shahbaz, T., Sansom, A. E., Naylor, T., & Dotani, T. 1994b, MNRAS, 268, 763
Smak, J. 1981, Acta Astron., 31, 395
Tanaka, Y., & Lewin, W. H. G. 1995, in X-Ray Binaries, ed. W. H. G. Lewin, J. van Paradijs, & E. P. J. van den Heuvel (Cambridge: Cambridge Univ. Press), 126
Thorsett, S. E., Arzoumanian, Z., McKinnon, M. M., & Taylor, J. H. 1993, ApJ, 405, L29
Tonry, J., & Davis, M. 1979, AJ, 84, 1511
Tsunemi, H., Kitamoto, S., Okamura, S., & Roussel-Dupré, D. 1989, ApJ, 337, L81
van den Heuvel, E. P. J. 1983, in Accretion-Driven Stellar X-Ray Sources, ed. W. H. G. Lewin & E. P. J. van den Heuvel (Cambridge: Cambridge Univ. Press), 303
van Paradijs, J., & McClintock, J. E. 1995, in X-Ray Binaries, ed. W. H. G. Lewin, J. van Paradijs, & E. P. J. van den Heuvel (Cambridge: Cambridge Univ. Press), 58
Wade, R. A., & Horne, K. 1988, ApJ, 324, 411
White, N. E., Nagase, F., & Parmar, A. N. 1995, in X-Ray Binaries, ed. W. H. G. Lewin, J. van Paradijs, & E. P. J. van den Heuvel (Cambridge: Cambridge Univ. Press), 1